Mathematical Problems in Engineering
Volume 4, pp. 21–42
Reprints available directly from the publisher
Photocopying permitted by license only

Shape Optimization of Turbine Blades with the Integration of Aerodynamics and Heat Transfer

J.N. RAJADAS[a], A. CHATTOPADHYAY[b,*], N. PAGALDIPTI[b] and S. ZHANG[b]

[a]*MAET Department,* [b]*Department of Mechanical and Aerospace Engineering, Arizona State University, Tempe, AZ 85287-6106, USA*

(Received 30 July 1996)

A multidisciplinary optimization procedure, with the integration of aerodynamic and heat transfer criteria, has been developed for the design of gas turbine blades. Two different optimization formulations have been used. In the first formulation, the maximum temperature in the blade section is chosen as the objective function to be minimized. An upper bound constraint is imposed on the blade average temperature and a lower bound constraint is imposed on the blade tangential force coefficient. In the second formulation, the blade average and maximum temperatures are chosen as objective functions. In both formulations, bounds are imposed on the velocity gradients at several points along the surface of the airfoil to eliminate leading edge velocity spikes which deteriorate aerodynamic performance. Shape optimization is performed using the blade external and coolant path geometric parameters as design variables. Aerodynamic analysis is performed using a panel code. Heat transfer analysis is performed using the finite element method. A gradient based procedure in conjunction with an approximate analysis technique is used for optimization. The results obtained using both optimization techniques are compared with a reference geometry. Both techniques yield significant improvements with the multiobjective formulation resulting in slightly superior design.

Keywords: Multidisciplinary; Optimization; Turbine blades; Aerodynamics; Heat transfer

* Corresponding author. Fax: 602-965-1384. E-mail: Chattopa@enws148.eas.asu.edu.

NOMENCLATURE

a_{le}	semi-major axis of leading edge ellipse
b_{le}	semi-minor axis of leading edge ellipse
C_t	tangential force coefficient
c_0, c_1, c_2, c_3	cubic spline coefficients
F	a performance function
f	an objective function
$\bar{f}$	prescribed target value of an objective function
h	convective coefficient
k	thermal conductivity of the blade
NCONT	number of thickness control points
NCONV	number of velocity control points
NDV	number of design variables
NPR	Prandtl number
NRE_ξ	Reynold's number based on ξ
T	blade temperature
t_k	airfoil thickness at the kth control point
VG_j	velocity gradient at jth control point
x	meridional coordinate
y	tangential coordinate
β_1	starting angle of leading edge ellipse
β_2	ending angle of leading edge ellipse
κ	thermal conductivity of air
Φ	design variable vector
ϕ_m	mth design variable
ξ	streamwise coordinate along airfoil
Ω	angle between major axis of leadingedge ellipse and meridional direction

Subscripts

ave	average value
l	lower bound
le	leading edge ellipse
∞	boundary value

INTRODUCTION

The design of turbine blades in gas turbine engines requires the integration of several important disciplines such as aerodynamics, heat transfer and structures [1,2]. The performance of the turbine is strongly coupled to its aerodynamic efficiency. The high temperature environment in the turbine affects the life of the blade and its structural integrity and efficient removal of heat from the blade interior will help in prolonging blade life. The method of heat removal also impacts the blade's structural integrity.

Improvement of the aerodynamic efficiency of the blade may be done in several ways. The primary method for achieving higher aerodynamic efficiency is the efficient design of the blade external shape. This involves the design of inlet and exit portions of the blade configuration such that there is a smooth and efficient transition between the blade channel and the free stream. This smooth transition is affected by the sharp velocity spikes associated with the blade leading edge on both the suction and the pressure surfaces (Fig. 1).

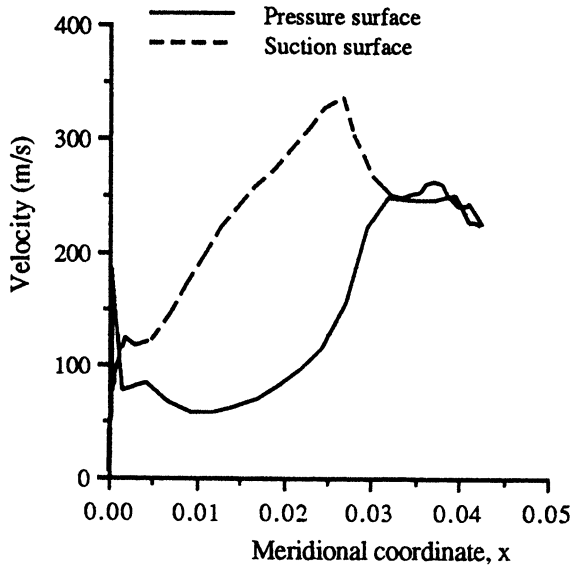

FIGURE 1 Velocity distribution for a typical blade section.

These velocity fluctuations can cause flow separation leading to poor aerodynamic performance. The aerodynamic efficiency of the blade can be greatly improved by eliminating such spikes. For a convectively cooled blade, the coolant path geometry of the blade is governed by the heat transfer between the external flow, the blade and the coolant. Due to allowable limits on material melting temperature and thermal stresses, both the external shape and the coolant path geometry must be designed such that the maximum and average temperatures in the blade are maintained as low as possible. Since the external flow heats up the blade, effective reduction in temperature can also be achieved by appropriate modification of the blade external shape. From a structural point of view, it is important to maintain the blade structure under allowable stress and vibration levels. Efficient turbine blade design therefore requires the integration of all of these disciplines.

Formal optimization techniques are being widely used in a variety of engineering design problems today. An extensive amount of work has been done in developing optimization procedures to bring the state of the art to a very high level [3]. The use of numerical optimization procedures for the design of airfoils has been a subject of considerable interest, primarily for wing design [4–8]. However, only limited information is available on applications of formal design optimization procedures for efficient turbine blade design. Chattopadhyay *et al.* [9] developed an optimization procedure for efficient aerodynamic design of turbine blades that successfully eliminated the leading edge velocity spikes without compromising blade performance. Dulikravich *et al.* [10–12] have developed inverse procedures for the design of blade coolant passages with specified temperatures and heat fluxes. However, the effect of blade external shape on heat transfer was not considered in these efforts. All of the above investigations were based on criteria related to a single discipline. However, a proper formulation of the design optimization problem must include the coupling of the necessary disciplines that impact the design to ensure realistic designs. Therefore, it is necessary to develop optimization procedures with multidisciplinary couplings.

In the present work, a multidisciplinary shape optimization procedure is presented for the design of turbine blades with the integration of aerodynamic and heat transfer criteria. To improve aerodynamic performance, it is desirable to eliminate the leading edge velocity

spikes (Fig. 1). The blade tangential force coefficient (C_t) is a measure of the torque produced by the turbine and hence, the work output of the turbine. During optimization, it is important to maintain the C_t value close to the reference value thus ensuring that there is no degradation in the work output of the turbine. It is also desirable to maintain the maximum and the average temperatures in the blade material as low as possible. In the present work, these requirements are appropriately incorporated into two multidisciplinary optimization problem formulations described in the next section. An appropriate model is developed for the blade section and the coolant path geometry. Since the aerodynamic performance is affected directly by the blade external shape and the heat transfer is affected by both the external shape as well as the coolant path geometry, the parameters defining the external shape and the coolant path geometry are used as design variables during optimization. Results from the two optimization procedures are compared.

OPTIMIZATION FORMULATION

Two different optimization formulations are investigated in the present study. The first represents a conventional single objective function and multiple constraints formulation. The second is a multiobjective formulation in which more than one design objective are included.

Single Objective Function Formulation

The maximum temperature in the blade section (T_{max}) which represents a measure of the heat transfer between the external fluid, the blade and the coolant, is used as the objective function to be minimized. Bounds are imposed on the velocity gradients at several control points along both the blade surfaces so that the leading edge velocity spikes are eliminated. A lower bound constraint is imposed on the tangential force coefficient (C_t) to maintain the aerodynamic efficiency of the blade at a desired level. It is also necessary to maintain the average temperature of the blade section (T_{ave}) below an allowable limit (T_{all}). Finally, to ensure that the procedure does not yield

aerodynamically infeasible designs, constraints are imposed on the airfoil thicknesses at various control points. Mathematically, the problem is stated as follows.

Minimize

Maximum blade temperature, $T_{\max}$

subject to

$$\begin{aligned}
&\mathrm{VG}_{j_1} \leq \mathrm{VG}_j \leq \mathrm{VG}_{j_u}, && j = 1, \ldots, \mathrm{NCONV},\\
&t_k \leq t_{k_u}, && k = 1, \ldots, \mathrm{NCONT},\\
&T_{\mathrm{ave}} \leq T_{\mathrm{all}},\\
&C_t \geq C_{t_{\min}},\\
&\phi_{m_1} \leq \phi_m \leq \phi_{m_u}, && m = 1, \ldots, \mathrm{NDV}.
\end{aligned}$$

Here, VG_j denotes the velocity gradient at the jth control point and the subscripts u and l represent upper and lower bounds, respectively. The quantity t_k denotes the airfoil thickness at the kth control point and ϕ_m represents the mth design variable. The quantities NCONV and NCONT denote the total number of velocity and thickness control points, respectively and NDV is the total number of design variables. In the present research, the velocity gradients at the control points are calculated using a forward finite difference approach. The magnitude of the velocities at two adjacent control points are differenced. This quantity is then divided by the difference in their x-coordinates to obtain the velocity gradients. The lower bounds for the velocity gradients are set to zero and the corresponding upper bounds are set to 10% of the magnitude of the velocity gradient of the reference blade at the corresponding control point.

Multiobjective Function Formulation

In this formulation, the average and maximum temperatures (T_{ave} and $T_{\max}$, respectively) are minimized simultaneously. Constraints on the tangential force coefficient (C_t) and the velocity gradients are imposed as in the single objective function formulation case. Since this formulation involves two objective functions, traditional optimization techniques based on single objective function cannot be used. In this paper, a multiobjective function formulation called the modified

global criteria approach developed by Chattopadhyay *et al.* [13] has been used. Using this approach, the two objective functions are combined into a single function as follows. Mathematically, if $f_1(\Phi)$ and $f_2(\Phi)$ are the two objective functions and $\bar{f}_1$ and $\bar{f}_2$ are their corresponding individually optimized values, then the global criteria function, $F(\Phi)$, is defined as follows:

$$F(\Phi) = \sqrt{(f_1 - \bar{f}_1)^2 + (f_2 - \bar{f}_2)^2}. \tag{1}$$

The global criteria function, $F(\Phi)$, represents the new objective function which is to be minimized. As can be inferred from Eq. (1), the minimization of $F(\Phi)$ forces the values of f_1 and f_2 towards their optimum values.

BLADE MODEL

In the present work, only two-dimensional aerodynamic and heat transfer analyses are carried out. Therefore, only the blade cross-sectional shape is considered. The blade external shape and coolant path cross sections are modeled as shown in Fig. 2. The suction surface and the pressure surface are represented by a series of cubic splines of the following form:

$$y = c_0 + c_1 x + c_2 x^2 + c_3 x^3, \tag{2}$$

where x is the meridional coordinate, y is the tangential coordinate and c_0, c_1, c_2 and c_3 are the spline coefficients. Continuity of function and slope are imposed at the end points of the splines. The tangential (y) coordinate and the slope of the surface at the spline joints on each surface are used as design variables in the optimization.

The flow field around the blade is significantly affected by the blade leading edge geometry. Hence, the blade leading edge shape and its effect on the aerodynamic efficiency is an important aspect of the shape optimization procedure. The leading edge geometry is modeled as an elliptic arc (Fig. 3) and is defined by its semi-major axis (a_{le}), semi-minor axis (b_{le}), starting and ending angles that define the elliptic arc (β_1 and β_2; angles BOD and AOD, respectively, in Fig. 3),

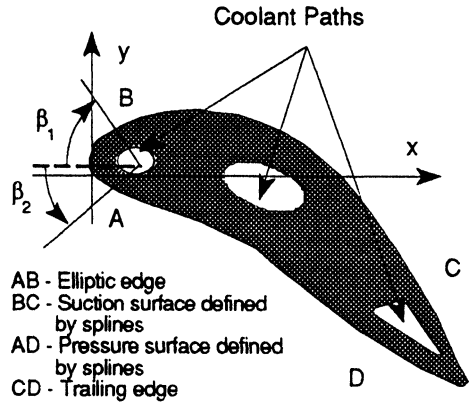

FIGURE 2 Blade model.

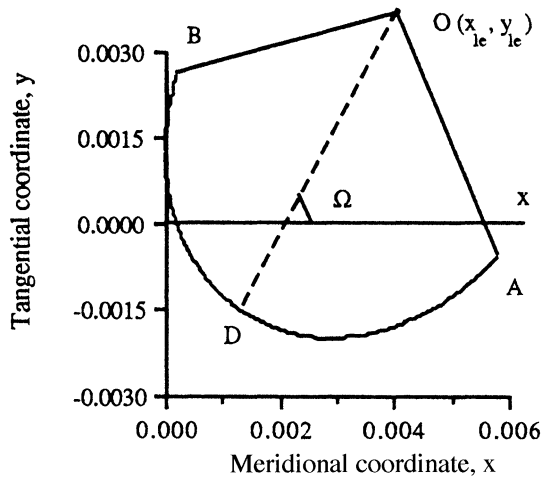

FIGURE 3 Elliptic leading edge.

orientation of the semi-major axis relative to the horizontal (Ω), meridional coordinate of the center O (x_{le}) and the tangential coordinate of the center O (y_{le}). In the present work, all the above parameters with the exception of x_{le} are used as design variables. The trailing edge shape is held fixed (same as reference blade) in order to satisfy the design requirement that the throat length of the turbine

blade cascade remain fixed. The chord length of the airfoil section along the x direction is also kept fixed. With the trailing edge fixed, the leading edge is required to be tangential to the station $y=0$ throughout the optimization ($y=0$ being the tangential coordinate of the leading edge of the reference blade section). This tangency requirement determines x_{le}. For elliptic leading edges, x_{le} is defined as follows:

$$x_{le} = a_{le}^2 \cos^2 \Omega + b_{le}^2 \sin^2 \Omega. \tag{3}$$

The first and the second coolant holes, located near the leading edge and the midsection of the blade, are defined using ellipses. The third coolant hole located near the trailing edge is triangular in shape. The first coolant ellipse has the same center as the outer surface, leading edge ellipse (Fig. 2). Its semi-major and semi-minor axes are included as design variables. The second coolant ellipse is defined by two x-stations which represent the left and the right extremes of the ellipse. The semi-major axis and orientation are determined by the thicknesses and the slopes of the blade section at these two x-stations. The two x values and semi-minor axis are included as design variables. The triangular coolant path is positioned in the trailing edge region based on the geometry of the airfoil trailing edge external surface. The x-coordinate of the right vertex and the height of the triangle are included as design variables.

ANALYSIS

The blade aerodynamic analysis is performed using a two-dimensional panel code developed by McFarland [14]. The code calculates compressible inviscid irrotational flow through a plane cascade of arbitrary blade shapes based on surface singularity methods. A simple forced convection model, based on a flat plate analysis [15], has been used to evaluate the convective coefficient of heat transfer between the external air and the blade. This model is as follows:

$$h_\xi = \frac{0.332(N_{PR})^{1/3}(N_{RE_\xi})^{1/2}\kappa}{\xi}, \tag{4}$$

where ξ represents the streamwise coordinate along the airfoil starting from the stagnation point, h_ξ is the local convective coefficient, N_{PR} is the Prandtl number of air, $N_{RE\xi}$ is the local Reynold's number based on the streamwise coordinate ξ, and κ is the thermal conductivity of air.

The temperature distribution in the interior of the blade is evaluated using a finite element procedure. In the multiply-connected blade section, it is formulated as the following scalar field problem:

$$\frac{\partial}{\partial x}\left(k\frac{\partial T}{\partial x}\right)+\frac{\partial}{\partial y}\left(k\frac{\partial T}{\partial y}\right)=0, \tag{5}$$

where T is the local blade temperature and k is the thermal conductivity of the blade material. Robin-type boundary conditions, based on the heat fluxes, are imposed on the blade external and internal boundaries as follows:

$$h(T-T_\infty)=k\bar{n}\cdot\text{grad}(T)=\text{Heat flux}, \tag{6}$$

where T_∞ is the local temperature of the air at the blade external and coolant boundary, h is the local coefficient of convectivity and $\bar{n}$ is the local outward normal to the boundary. The boundary value problem is numerically solved using the finite element method. The computational domain is discretized using linear triangular elements. Figure 4 presents a typical computational mesh used in the finite element analysis. Since the geometry of the blade changes during optimization, an adaptive mesh generation technique has been used. Using the Galerkin approach, the above boundary value problem (Eqs. (5) and (6)) is reduced to the following system of linear simultaneous equations for the unknown nodal temperatures:

$$[K]\bar{T}=\bar{R}. \tag{7}$$

Here, the coefficient matrix, $[K]$ and the right hand side vector, $\bar{R}$, are evaluated using the finite element formulation and the boundary conditions. The solution of Eq. (7) yields the nodal temperatures, $\bar{T}$.

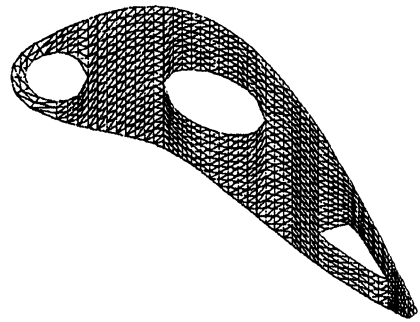

FIGURE 4 Finite element mesh.

OPTIMIZATION STRATEGY

In both the single objective and the multiobjective function formulations, the optimization is performed using the method of feasible directions [16]. The design sensitivities are calculated using finite difference techniques. In a gradient-based optimization several evaluations of the objective function and the constraints are necessary. The use of exact analysis to evaluate these at each iteration iscomputationally expensive. Hence an approximation technique, known as the two-point exponential approximation [17] is used. In this technique, the exponent used in the expansion is based upon the gradient information from the previous and current design cycles. This technique is formulated as follows:

$$\hat{F}(\Phi) = F(\Phi_1) + \sum_{n=1}^{\text{NDV}} \left[\left(\frac{\Phi_n}{\Phi_{1_n}} \right)^{p_n} - 1.0 \right] \frac{\Phi_{1_n}}{p_n} \frac{\partial F(\Phi_1)}{\partial \Phi_n}, \tag{8}$$

where $\hat{F}(\Phi)$ is the approximation of the function $F(\Phi)$. The exponent, p_n, is defined below:

$$p_n = \frac{\log_e \left\{ \dfrac{(\partial F(\Phi_0)/\partial \Phi_n)}{\partial F(\Phi_1)/\partial \Phi_n} \right\}}{\log_e \{\Phi_{0_n}/\Phi_{1_n}\}} + 1.0. \tag{9}$$

The quantity Φ_0 refers to the design variable vector from the previous optimization cycle and the quantity Φ_1 denotes the current design vector. A similar expression is derived for the constraint vector. Equation (8) indicates that in the limiting case of $p_n = 1$, the expansion is identical to the traditional first order Taylor series and when $p_n = -1$, the two-point exponential approximation reduces to the reciprocal expansion form. The exponent is then defined to lie within the interval, $-1 \leq p_n \leq 1$. If $p_n > 1$, it is set identically equal to one and if $p_n < -1$, it is set equal to -1. The exponent p_n can then be considered as a "goodness of fit" parameter, which explicitly determines the trade-off between traditional and reciprocal Taylor series based expansions, resulting in a hybrid approximation technique.

RESULTS

The two optimization procedures described above are used to optimize an existing turbine blade geometry [14]. The reference geometric configuration is defined by the set of geometric parameters (design variables) presented in Tables I and II. Two splines have been used on both the suction and pressure surfaces of the blade. The two splines join at a meridional coordinate, $x = 0.020$ m. The blade external shape is discretized into 70 panels. The panel code uses this discretized blade geometry and evaluates the flow field around it. The blade interior is discretized using approximately 600 nodes resulting in approximately 1000 finite elements. Since an adaptive mesh generation procedure is used to generate the finite element mesh, the discretization of the computational domain changes during the optimization. In the calculation of the coefficient of convective heat transfer (Eq. (4)) between the external flow and the blade, the value of the Prandtl number (N_{PR}) is 0.72, the kinematic viscosity of air is $9.1 \times 10^{-5}\,m^2/s$ and the thermal conductivity of air (κ) is 0.06115 W/m-°C. The thermal conductivity of the blade material (k) is 34.62 W/m-°C and the coolant temperature is 300°C. In the multiobjective function formulation, the values of $\bar{f}_1$ and $\bar{f}_2$ (Eq. (1)) are set to zero thus providing the optimizer with greater flexibility.

Figure 5 shows the comparison between the reference and the optimum values of the maximum and average temperatures in the

TABLE I Blade leading edge design variables

Design variable	*Reference*	*Optimum*	
		Single obj. function	*Modified global criteria*
Semi-major axis of outer ellipse, a_{leo}	3.4075E−03 m	4.8285E−03 m	4.2594E−03 m
Semi-minor axis of outer ellipse, b_{leo}	4.4918E−03 m	6.0574E−03 m	5.6147E−03 m
Semi-major axis of inner ellipse, a_{lei}	1.5670E−03 m	3.2992E−03 m	2.5556E−03 m
Semi-minor axis of inner ellipse, b_{lei}	2.1714E−03 m	3.9613E−03 m	3.3369E−03 m
Starting angle of elliptic arcs, β_1	60.7°	60.7°	60.7°
Ending angle of elliptic arcs, β_2	62.7°	62.7°	62.7°
Orientation of the semi-major axis, Ω	−1.4467E−06°	−1.4467E−06°	−1.4467E−06°
Tangential (y) coordinate of ellipse center, y_{le}	1.3852E−06 m	1.3852E−06 m	1.3852E−06 m

TABLE II Blade coolant path geometry and spline variables

Design variable	*Reference*	*Optimum*	
		Single obj. function	*Modified global criteria*
x-coordinate of second coolant path's left point	1.8000E−02 m	1.9124E−02 m	1.7520E−02 m
x-coordinate of second coolant path's right point	2.2000E−02 m	2.3774E−02 m	2.3426E−02 m
Semi-minor axis of second coolant path	2.5000E−03 m	3.8959E−03 m	4.0000E−03 m
Height of third coolant path (triangular hole)	4.0000E−03 m	5.0054E−03 m	5.0000E−03 m
x-coordinate of third coolant path's right point	3.9000E−02 m	4.0005E−02 m	4.0241E−02 m
y-coordinate of upper-outer splines at $x = 0.02$ m	6.3111E−03 m	9.9309E−03 m	7.7301E−03 m
Slope of upper-outer splines at $x = 0.02$ m	−5.4625E−01	−5.4618E−01	−5.46229E−01
y-coordinate of lower-outer splines at $x = 0.02$ m	−1.6035E−02 m	−1.4760E−02 m	−1.5442E−02 m
Slope of lower-outer splines at $x = 0.02$ m	−1.1799E+00	−1.1797E+00	−1.1797E+00

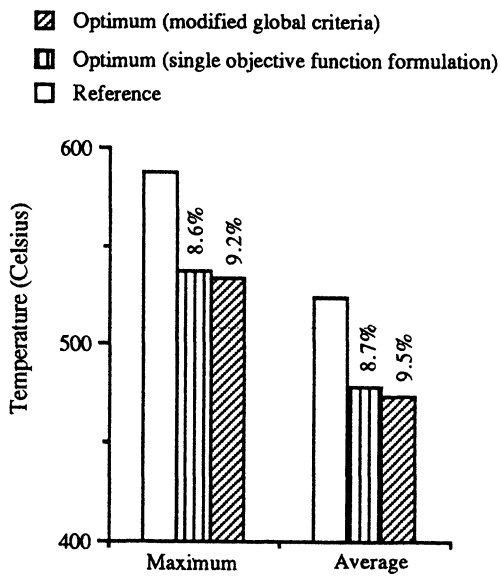

FIGURE 5 Comparison of blade temperatures.

blade section. For the reference configuration, the maximum temperature (T_{max}) is 588°C and the average temperature (T_{ave}) is 537°C. Both optimization procedures yield significant reductions in these quantities. Using the single objective function optimization formulation, the maximum temperature has been reduced by 8.6% and the average temperature has been reduced by 8.7%. The modified global criteria approach results in better improvements. The maximum temperature has been reduced by 9.2% and the average temperature has been reduced by 9.4%. These reductions are due to significant changes in the external and the coolant path geometry of the blade after optimization. Figures 6(a) and (b) compare the reference geometry and the optimum geometries obtained using the single objective function formulation and the modified global criteria approach respectively. It can be seen that the external shape and the coolant path geometries have been modified by both the optimization procedures. Further, it is to be noted that the optimum configurations yielded by the two optimization formulations are different. In the modified global criteria approach, the blade average temperature is included as an objective

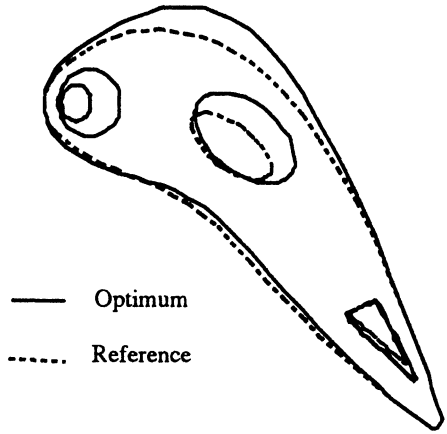

FIGURE 6(a) Comparison of airfoil geometry; single objective function formulation.

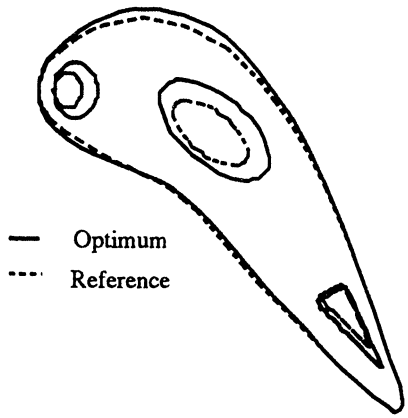

FIGURE 6(b) Comparison of airfoil geometry; modified global criteria formulation.

function. Unlike the blade maximum temperature which is a local quantity, the blade average temperature is a global quantity. Its inclusion in the optimization formulation forces the optimizer towards designs which have cooler temperatures through out the entire blade section. Due to this reason, the modified global criteria approach yields a slightly improved optimum over the single objective function formulation. However, there are some features common to the results

from both procedures. The coolant paths in all the three regions have increased in area. This increase in the coolant path cross-sectional areas causes more heat to be removed from the blade leading to a favorable redistribution of the blade temperature. The temperature distribution of the reference blade is presented in Fig. 7(a) and the corresponding distributions for the optimum configurations are

FIGURE 7(a) Temperature distribution for the reference blade.

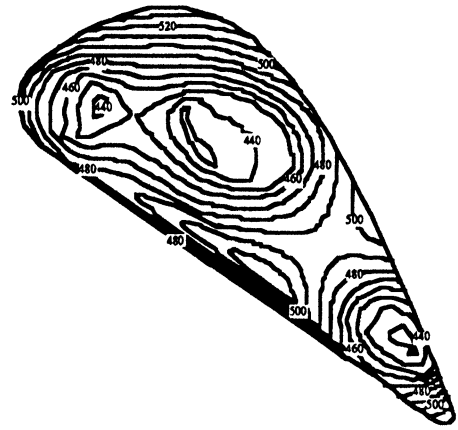

FIGURE 7(b) Temperature distribution for the optimum blade; single objective function formulation.

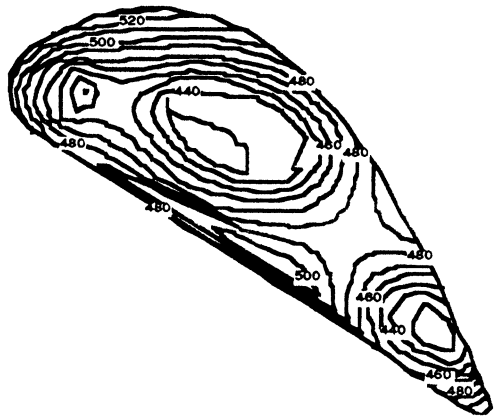

FIGURE 7(c) Temperature distribution for the optimum blade; modified global criteria formulation.

presented in Figs. 7(b) and (c) respectively. The favorable redistribution of temperature in the optimum configurations can be seen from these figures. The modified global criteria approach yields more reduction in the maximum and average temperatures than the single objective optimization formulation because the former approach yields an optimum design with bigger coolant areas than the latter formulation.

Figure 8 compares the tangential force coefficients of the reference and optimum blades. In spite of the significant changes to the blade external shape, both the optimization procedures maintain the tangential force coefficient at the reference value. The tangential force coefficient was introduced as a constraint in the single objective function formulation. It must be noted that this constraint represents a critical constraint in the optimization. The velocity distributions for the reference and optimum configurations are presented in Figs. 9(a) and (b). The reference blade velocity profile exhibits a sharp spike on the suction surface. In the optimum configurations, this spike is eliminated using both single and multiobjective procedures. The leading edge geometry, which is crucial in the determination of the velocity distribution, has changed significantly. This is seen in Table I as well as Figs. 6(a) and (b). However, the starting and ending angles (β_1 and β_2), the orientation of the semi-major axis relative to the horizontal (Ω) and the tangential coordinate of the center of the leading edge elliptic

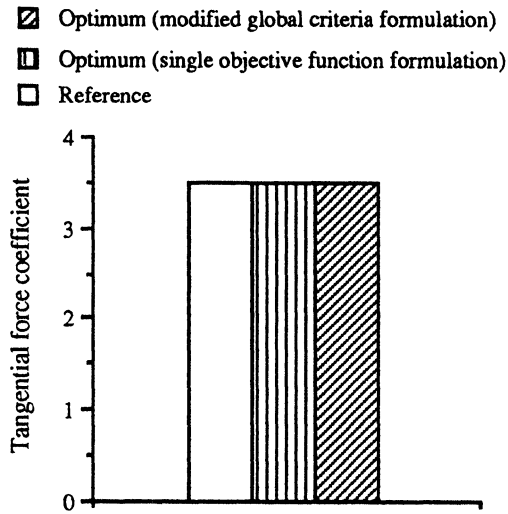

FIGURE 8 Comparison of tangential force coefficient.

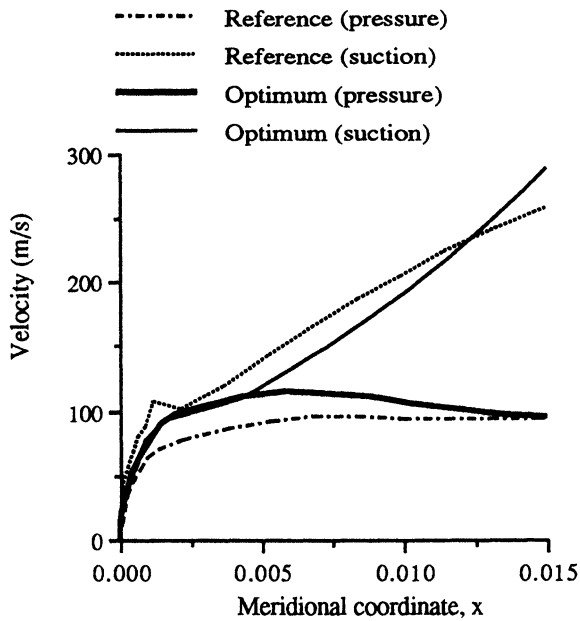

FIGURE 9(a) Comparison of velocity distributions; single objective function formulation.

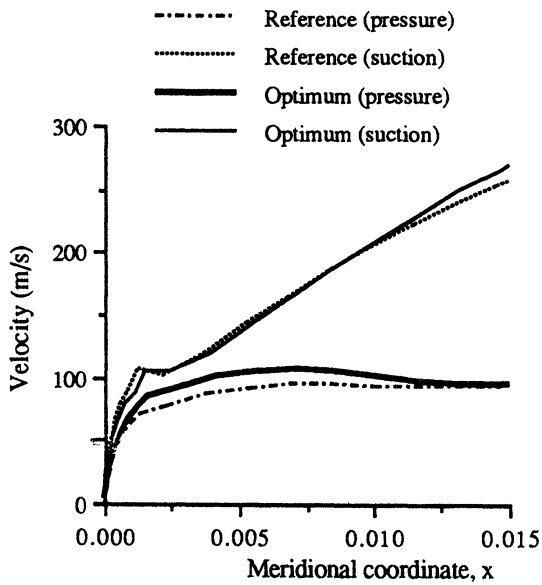

FIGURE 9(b) Comparison of velocity distributions; modified global criteria formulation.

arc (y_{le}) have not undergone any significant changes during the optimizations. This indicates that these variables do not influence the optimization as significantly as the other design variables that have undergone significant changes during the optimization. Due to the relatively low sensitivity of the design to these parameters, they can be removed from the set of design variables, thus improving the computational efficiency of the optimization procedures.

Both single objective function formulation as well as multiobjective function formulation yield significant reduction in the blade temperatures and successfully eliminate the leading edge spikes. However, the optimum solutions from the two techniques exhibit some differences. The optimum configuration obtained from the single objective function formulation shows more increase in the leading edge thickness of the airfoil than the optimum configuration obtained from the multiobjective function formulation. This results in a relatively smoother optimum velocity distribution for the former case. The optimum temperatures obtained using the multiobjective function formulation

are slightly lower than the optimum temperatures from the single objective function formulation because the coolant hole areas are slightly higher in the former case. The single objective function optimization procedure converges in 39 optimization cycles whereas the multiobjective function formulation converges in 12 optimization cycles. Each optimization cycle requires approximately 20 s of CPU time on a Sun workstation. Thus, the single objective function optimization procedure requires nearly 800 s while the multiobjective function formulation coverges in 250 CPU seconds. This clearly indicates that the multiobjective function formulation using the modified global criteria approach is computationally superior to the single objective function formulation technique.

CONCLUDING REMARKS

A multidisciplinary optimization procedure, with the integration of aerodynamic and heat transfer criteria, has been developed for the design of gas turbine blades. Two different optimization formulations have been used to study the design problem. The single objective formulation uses the maximum blade temperature as the objective function and imposes an upper bound on the average blade temperature and a lower bound on the tangential force coefficient. The multiobjective function formulation uses the maximum and average blade temperatures as objective functions. A lower bound is imposed on the tangential force coefficient as in the single objective function formulation. In both formulations, upper and lower bound constraints are imposed on the velocity gradients at several points along the blade pressure and suction surfaces to eliminate velocity spikes. A panel code is used for aerodynamic analysis and the finite element method is used for heat transfer analysis. The following observations are made from this study.

1. Both optimization procedures are very effective in modifying the blade external and coolant path geometries and yield significant reductions in maximum and average temperatures of the blade.
2. The optimization procedures effectively eliminate leading edge velocity spikes and maintain aerodynamic performance at the reference value.

3. The reductions in the blade temperature are due to the redistribution of temperature in the blade section, caused by the increase in the coolant areas and the changes to the external shape. The elimination of the leading edge velocity spikes is due to the significant change in the leading edge geometry.
4. The starting and ending angles, the orientation of the semi-major axis and the tangential coordinate of the leading edge elliptic arc do not change during optimization and are possible candidates for design variable elimination.
5. The multiobjective function formulation using the modified global criteria approach yields slightly improved blade temperatures.
6. Faster convergence to optimum design is achieved using the multiobjective formulation.

Acknowledgments

This research was supported by Allied Signal Aerospace Company, Grant Number AH51001, Technical Monitor, Mr. Thomas Elliot. The authors would also like to acknowledge the technical support of Dr. David Winstanley.

References

[1] Glassman, A.J., *Turbine Design and Application*, Vols. 1 and 2, NASA SP 290, 1972.
[2] Civinkas, K.C., Impact of ETO propellents on the aerothermodynamic analyses of propulsion components, AIAA Paper No. 83-3091, Presented at the *ÀIAA/ASME/SAE/ASEE 24th Joint Propulsion Conference*, Boston, Massachusetts, 1988.
[3] Ashley, H. On making things the best – Aeronautical use of optimization, *AIAA Journal of Aircraft*, **19**(1), 1982.
[4] Hague, D.S., Rozendaal, H.L. and Woodward, F.A., Application of multivariable search techniques to optimal aerodynamic shaping problems, *Journal of Aerospace Sciences*, **15**(6), November–December, 1968, 283–296.
[5] Vanderplaats, G.N., Hicks, R.M. and Murman, E.M., Application of numerical optimization techniques to airfoil design, *Proc. Aerodynamic Analyses Requiring Advanced Computers, Part II*, Langley Research Center, Hampton, Virginia, 1975.
[6] Vanderplaats, G.N. and Hicks, R.M., Numerical airfoil optimization using a reduced number of design coordinates, NASA TMX-73, 151, 1976.
[7] Jameson, A., Aerodynamic design via control theory, *Journal of Scientific Computing*, **3**, 1988, 233–260.
[8] I-Chung, Chang and Torres, F.J., Wing design code using three dimensional Euler equations and optimization, *AIAA Aircraft Design Systems and Operations Meeting*, Baltimore, Maryland, 1991.
[9] Chattopadhyay, A., Pagaldipti, N. and Chang, K.T., A design optimization procedure for efficient turbine airfoil design, *Journal of Computers and Mathematics with Applications*, **26**(4), 1993, 21–31.

[10] Kennon, S.R. and Dulikravich, G.S., The inverse design of internally cooled turbine blades, *Journal of Engineering for Gas Turbines and Power*, **107**, January 1985, 123–126.
[11] Dulikravich, G.S. and Martin, T.J., Inverse design of super elliptic coolant passages in coated turbine blades with specified temperatures and heat fluxes, AIAA Paper No. 92-4714, *4th AIAA/USAF/NASA/OAI Symposium on Multidisciplinary Analysis and Optimization*, Cleveland, Ohio, 1992.
[12] Dulikravich, G.S. and Martin, T.J., Three-dimensional coolant passage design for specified temperature and heat fluxes, AIAA Paper No. 94-0348, *32nd Aerospace Sciences Meeting and Exhibit*, Reno, Nevada, 1994.
[13] Chattopadhyay, A., Walsh, J.L. and Riley, M.F., Integrated aerodynamic/dynamic optimization of helicopter blades, *Proceedings of the AIAA/ASME/ASCE/AHS 30th Structures, Structural Dynamics and Materials Conference*, Mobile, Alabama, 1989. AIAA Paper No. 89-1269. Also available as NASA TM-101553, February, 1989.
[14] McFarland, E.R., Panel code for 2d blade to blade solutions, *NASA TMX-81589*.
[15] Chapman, A.J., *Heat Transfer*, Third Edition, Macmillan Publishing Co., Inc., 1974.
[16] Vanderplaats, G.N., CONMIN – A FORTRAN program for constrained function minimization, Users Manual, NASA TMX-62282, July, 1987.
[17] Fadel, G.M., Riley, M.F. and Barthelemy, J.F.M., Two-point exponential approximation method for structural optimization, *Structural Optimization*, **2**, 1990, 117–124.

Mathematical Problems in Engineering

Special Issue on Time-Dependent Billiards

Call for Papers

This subject has been extensively studied in the past years for one-, two-, and three-dimensional space. Additionally, such dynamical systems can exhibit a very important and still unexplained phenomenon, called as the Fermi acceleration phenomenon. Basically, the phenomenon of Fermi acceleration (FA) is a process in which a classical particle can acquire unbounded energy from collisions with a heavy moving wall. This phenomenon was originally proposed by Enrico Fermi in 1949 as a possible explanation of the origin of the large energies of the cosmic particles. His original model was then modified and considered under different approaches and using many versions. Moreover, applications of FA have been of a large broad interest in many different fields of science including plasma physics, astrophysics, atomic physics, optics, and time-dependent billiard problems and they are useful for controlling chaos in Engineering and dynamical systems exhibiting chaos (both conservative and dissipative chaos).

We intend to publish in this special issue papers reporting research on time-dependent billiards. The topic includes both conservative and dissipative dynamics. Papers discussing dynamical properties, statistical and mathematical results, stability investigation of the phase space structure, the phenomenon of Fermi acceleration, conditions for having suppression of Fermi acceleration, and computational and numerical methods for exploring these structures and applications are welcome.

To be acceptable for publication in the special issue of Mathematical Problems in Engineering, papers must make significant, original, and correct contributions to one or more of the topics above mentioned. Mathematical papers regarding the topics above are also welcome.

Authors should follow the Mathematical Problems in Engineering manuscript format described at http://www.hindawi.com/journals/mpe/. Prospective authors should submit an electronic copy of their complete manuscript through the journal Manuscript Tracking System at http://mts.hindawi.com/ according to the following timetable:

Manuscript Due	March 1, 2009
First Round of Reviews	June 1, 2009
Publication Date	September 1, 2009

Guest Editors

Edson Denis Leonel, Department of Statistics, Applied Mathematics and Computing, Institute of Geosciences and Exact Sciences, State University of São Paulo at Rio Claro, Avenida 24A, 1515 Bela Vista, 13506-700 Rio Claro, SP, Brazil; edleonel@rc.unesp.br

Alexander Loskutov, Physics Faculty, Moscow State University, Vorob'evy Gory, Moscow 119992, Russia; loskutov@chaos.phys.msu.ru